Recent progress in rigorous algorithms for the fast solution of 3-D EM frequency-domain integral-equations

Anton Menshov[1], Yaniv Brick[1], Carlos Torres-Verdín[1], and Ali E. Yilmaz[1]
[1]The University of Texas at Austin

SUMMARY

We introduce a fast iterative and a fast direct algorithm for rapid solution of frequency-domain integral-equation formulations pertinent to 3-D electromagnetic modelling and inversion. The iterative algorithm is based on the adaptive integral/pre-corrected FFT method: It accelerates the matrix-vector products at each iteration by enclosing the arbitrary primary mesh of the anomalous domain of interest with a single auxiliary regular grid, approximating interactions among basis and testing functions via grid-based anterpolation, propagation, and interpolation, using 3-D FFTs to multiply grid-to-grid propagation matrices with vectors, and pre-correcting inaccurate approximations for nearby interactions. The direct algorithm is based on a $\mathcal{H}$-matrix framework: it accelerates the matrix factorization by constructing a hierarchy of matrix blocks that represent interactions between pairs of subdomains, compressing admissible interactions between well-separated subdomains with localized auxiliary regular grids, computing low-rank approximations of grid-to-grid propagation matrices, and using $\mathcal{H}$-matrix arithmetic. The performance of the two algorithms is compared for computing the electromagnetic response of propped hydraulic fractures. Distributed-memory parallelization of the iterative algorithm, which has recently been scaled up to solve large-scale problems with $>10^9$ degrees of freedom using $>10^4$ processes, enables effective calculation of the response of very complex and large-scale fractures. The direct algorithm remains accurate, however, even as (a) the fracture conductivity increases relative to the background, (b) the conditioning of the system of equations and the convergence of its iterative solution deteriorates, and (c) the fast iterative algorithm fails to yield accurate results.

Keywords: integral equation methods, forward modelling, iterative algorithms, direct algorithms, hydraulic fractures

INTRODUCTION

Robust algorithms for rapid numerical solution of frequency-domain integral-equation formulations that arise from 3-D electromagnetic modelling and inversion have been of interest in applied geophysics, geophysical exploration, formation evaluation, and remote sensing for more than four decades (Hohmann, 1975).

Despite the steady advances in computational science and engineering over this period, including vast improvements in parallel hardware and software infrastructure, the rigorous method of moments (MoM) solution of integral equations remains limited to small-scale simulations. This is in great part because of the (i) high computational costs of solving dense linear systems—using classical LU decomposition to solve the system of equations requires $\mathcal{O}(N^3 + N_{\text{rhs}}N^2)$ operations and $\mathcal{O}(N^2)$ memory, where N is the number of unknowns used to discretize the currents/fields on/in anomalous regions and N_{rhs} is the number of different excitations, (ii) poor conditioning of the system of equations that deteriorates due to various factors (e.g., dense discretization, low frequency, high conductivity contrast), and (iii) difficulty of computing singular Green's functions and their integrals accurately for complex backgrounds.

Over the last decade, a variety of algorithms have been advanced to address the above challenges and accelerate the MoM solution of frequency-domain integral equations. In this paper, an FFT-based fast iterative and an $\mathcal{H}$-matrix based fast direct algorithm are contrasted in the context of forward modelling of hydraulic fracture detection via borehole resistivity measurements.

FORMULATION

Consider an arbitrarily shaped inhomogeneous anomalous 3-D volume V in an unbounded homogeneous background excited by the time-harmonic electromagnetic field $\{\mathbf{E}^{\text{inc}}, \mathbf{H}^{\text{inc}}\}$ generated by impressed sources ($e^{j\omega t}$ time variation is assumed and suppressed). For simplicity, assume that the {anomalous volume, background} are non-magnetic isotropic materials with permeability μ_0 and complex permittivity $\{\tilde{\varepsilon}_V, \tilde{\varepsilon}_b\} = \{\varepsilon_V, \varepsilon_b\} + \{\sigma_V, \sigma_b\} / j\omega$; the following formulation and methods can be extended to magnetodielectric (Yu et al., 2014) and anisotropic (Yang et al., 2013) anomalies as well as uniaxial layered backgrounds (Yang et al., 2013).

To compute the secondary fields generated by the anomalous volume, the volume electric field integral equation (VEFIE) is constructed by relating the total electric field to the conduction-current corrected electric flux density $\tilde{\mathbf{D}}$ induced in V as (Yang et al., 2015)

$$\mathbf{E}^{\mathrm{inc}}(\mathbf{r}) = \frac{\tilde{\mathbf{D}}(\mathbf{r})}{\tilde{\varepsilon}_{\mathrm{V}}(\mathbf{r})} - \mathbf{E}^{\mathrm{sca}}(\mathbf{r}) \qquad \text{for } \mathbf{r} \in V \tag{1}$$

and expressing the secondary fields as

$$\mathbf{E}^{\mathrm{sca}}(\mathbf{r}) = \iiint\limits_{V} [\omega^2 \mu_0 g(R) + \frac{\nabla g(R)}{\tilde{\varepsilon}_{\mathrm{b}}} \nabla' \cdot] \chi(\mathbf{r}') \tilde{\mathbf{D}}(\mathbf{r}') \ dv' \tag{2}$$

where $R = \left| \mathbf{r} - \mathbf{r}' \right|$ is the distance between the source and observer points, $g(R) = e^{-\gamma_{\mathrm{b}} R} / 4\pi R$ is the Green's function for the homogeneous background, $\gamma_{\mathrm{b}} = j\omega\sqrt{\mu_0 \tilde{\varepsilon}_{\mathrm{b}}}$ is the complex propagation constant in the background, and $\chi(\mathbf{r}) = 1 - \tilde{\varepsilon}_{\mathrm{b}} / \tilde{\varepsilon}_{\mathrm{V}}(\mathbf{r})$ is the complex contrast ratio.

Method of Moments (MoM) Solution

The VEFIE is converted to a systems of linear equations by (i) meshing V in terms of tetrahedral elements that have a total of N triangular faces, (ii) expanding $\tilde{\mathbf{D}}$ using N SWG functions $\mathbf{f}_1, \ldots, \mathbf{f}_N$ (Schaubert et al., 1984), and (iii) testing the resulting equations with $\chi_1 \mathbf{f}_1, \ldots, \chi_N \mathbf{f}_N$ (Yang et al., 2013). This MoM procedure yields the matrix equation

$$\mathbf{Z}_{N \times N} \mathbf{I}_{N \times N_{\mathrm{rhs}}} = \mathbf{V}^{\mathrm{inc}}_{N \times N_{\mathrm{rhs}}} \tag{3}$$

Here, $\mathbf{Z}$ is the dense MoM impedance matrix, $\mathbf{I}$ is the matrix of unknown coefficients, and $\mathbf{V}^{\mathrm{inc}}$ is the matrix that stores tested incident fields. This linear system of equations can be solved by using classical general-purpose iterative or direct solvers. Both categories of solvers, however, quickly become inappropriate because they suffer from the difficulties listed in the Introduction.

FAST ALGORITHMS

Fast iterative or direct algorithms can be used to reduce the high computational costs of the MoM solution.

Iterative Algorithm

A large variety of iterative solution methods that are accelerated by fast matrix-vector multiplications are available for reducing computational costs. For example, FFT-based algorithms for regularly (Fang et al., 2006, Yu et al., 2014) or irregularly meshed regions (Nie et al., 2010, Yang et al., 2015), their massively parallel versions (Wei et al., 2014), and their extensions to anomalies residing in planar-layered backgrounds (Yang et al., 2012, 2013) can reduce computational costs significantly and enable the analysis of extremely complex and large-scale forward models. Indeed, for a large variety of conditions, such algorithms reduce the computational costs to $\mathcal{O}(\bar{N}_{\mathrm{iter}} N_{\mathrm{rhs}} N \log N)$ operations

and $\mathcal{O}(N)$ memory requirement, where $\bar{N}_{\mathrm{iter}}$ is the average number of iterations needed for convergence. In this paper, we invoke the pre-corrected FFT/adaptive integral method (AIM) detailed in (Yang et al., 2015).

Direct Algorithm

Iterative solution methods become less effective, however, as the conditioning of the system of equations deteriorates, e.g., as $\tilde{\varepsilon}_{\mathrm{V}}$ increases. Preconditioners can help delay the eventual breakdown (Nie et al., 2012, Fang et al., 2006); alternatively, direct solution methods can be used (Menshov et al., 2015, 2016).

While for high-frequency wave propagation and scattering problems compression is more limited (Brick et al., 2016), for low-frequency problems, and particularly in lossy/diffusive backgrounds, several classes of algorithms can efficiently yield a compressed representation of the impedance matrix. In this paper, we use a fast direct solver based on the $\mathcal{H}$-matrix framework (Hackbusch, 1999). This approach relies on the hierarchical partitioning of the impedance matrix into blocks corresponding to interactions between clusters of basis and testing functions. In the matrix partitioning process, blocks that correspond to sufficiently separated clusters are considered "admissible" and, instead of being explicitly constructed and stored, are represented using a low-rank (LR) approximation. Blocks that do not satisfy the distance-based admissibility criterion are further partitioned. The process continues until blocks associated with sufficiently small basis/testing function clusters are reached; the latter are computed and stored directly. Once the $\mathcal{H}$-matrix is computed, its particular compressed structure enables the application of a special $\mathcal{H}$-matrix arithmetic for its fast hierarchical-LU ($\mathcal{H}$-LU) factorization and then forward/backward substitutions.

In our fast direct solver implementation, the LR representation of impedance matrix blocks are computed by using auxiliary grids. Rather than directly generating impedance matrix blocks and compressing them algebraically, e.g., by using the singular value decomposition (SVD), the interactions between basis and testing functions are approximated by a product of smaller and sparser matrices. To that end, each source cluster s and observer cluster o are enclosed by regular grids whose grid spacings are dictated by the background penetration depth. The $N_o \times N_s$ matrix block $\mathbf{Z}^{os}$ is approximated as

$$\mathbf{Z}^{os} \approx \sum_{i \in \{\mathrm{x,y,z,\nabla}\}} \left(\Lambda_o^i \right)^T \mathbf{G}^{os} \Lambda_s^i \tag{4}$$

where $\mathbf{G}^{os}$ is an $N_o^{\mathrm{g}} \times N_s^{\mathrm{g}}$ grid-to-grid propagation matrix and $\Lambda_{o,s}^i$ are $N_{o,s}^{\mathrm{g}} \times N_{o,s}$ anterpolation (adjoint
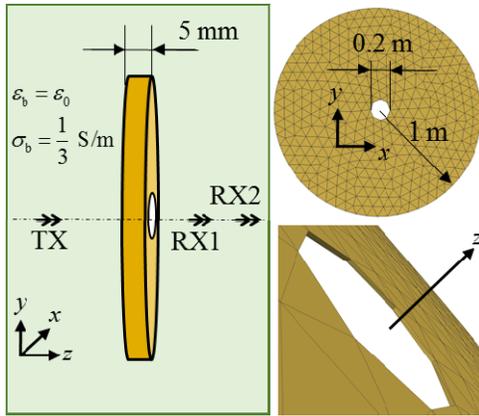
Figure 1. EM detection of a propped hydrofracture. Model and tetrahedral mesh used in the simulations.

interpolation) matrices found by moment matching. To obtain a LR approximation of $\mathbf{Z}^{os}$, the SVD

$$\mathbf{G}^{os} = \mathbf{U}\Sigma\mathbf{V}^{H} \qquad (5)$$

is computed and truncated according to a prescribed threshold τ_{SVD}. Keeping only the singular values on the diagonal of Σ that are greater than τ_{SVD} times the largest singular value and the corresponding columns of $\mathbf{U}$ and $\mathbf{V}$, and denoting the truncated SVD as $\mathbf{G}^{os} \approx \hat{\mathbf{U}}\hat{\Sigma}\hat{\mathbf{V}}^{H}$, the LR approximation is given as

$$\mathbf{Z}^{os} \approx \underbrace{\left[\Lambda_o^{xT}\hat{\mathbf{U}}\hat{\Sigma} \quad \Lambda_o^{yT}\hat{\mathbf{U}}\hat{\Sigma} \quad \Lambda_o^{zT}\hat{\mathbf{U}}\hat{\Sigma} \quad \Lambda_o^{\nabla T}\hat{\mathbf{U}}\hat{\Sigma} \right]}_{\mathbf{A}} \underbrace{\begin{bmatrix} \hat{\mathbf{V}}^H \Lambda_s^x \\ \hat{\mathbf{V}}^H \Lambda_s^y \\ \hat{\mathbf{V}}^H \Lambda_s^z \\ \hat{\mathbf{V}}^H \Lambda_s^\nabla \end{bmatrix}}_{\mathbf{B}^H} \qquad (6)$$

NUMERICAL RESULTS

The capabilities of FFT-based fast iterative algorithms have been amply demonstrated in the literature (Fang et al., 2006, Yu et al., 2014, Nie et al., 2010, Wei et al., 2014, Yang et al., 2012, 2013, 2015). Here, one shortcoming of these algorithms is highlighted (the high-contrast breakdown), and the benefit of using the $\mathcal{H}$-matrix based fast direct algorithm is demonstrated.

Model

Resistivity measurements acquired with a coaxial induction logging tool are modelled along a horizontal open-hole penetrating a 3-D hydro-fracture in a homogeneous shale formation, as shown in Fig. 1. Just as in (Yang et al., 2015), the transmitter is modelled as a point source—a unit z-oriented impressed magnetic Hertzian dipole located on the borehole axis—and two z-oriented receiver coils are located $d_1 = 1.2\ \text{m}$ and $d_2 = 1.5\ \text{m}$ away. A small fracture is modelled as a 1-m radius and 5-mm thin symmetrical cylindrical disk that

starts outside the 0.1-m radius borehole. The effective conductivity of the fracture is a parameter whose effects are investigated. Unlike (Yang et al., 2015), the mandrel and the mud-column are not included in the model; instead the borehole is replaced with the background formation because its influence was found to be negligible for coaxial induction measurements (Zhang et al., 2016). The irregular tetrahedral mesh of the fracture resulted in $N = 5284$ unknowns. In the following simulations, the logging tool is assumed to operate at 100 Hz and to be moved such that the center of the receivers is at most 3 m in front or behind the center of the fracture. At each tool position, the total magnetic field at each receiver axis is computed and processed to find the voltages detected at the two receivers; these voltages are then linearly combined to reduce the contribution of the incident field to the detected signal as

$$\Delta U_{\text{frac}}^{zz} = -j\omega\mu_0\hat{\mathbf{z}}\cdot\left[\mathbf{H}^z(\mathbf{r}_{\text{RX2}}) - \mathbf{H}^z(\mathbf{r}_{\text{RX1}})d_1^3 / d_2^3\right] (\text{V}) \qquad (7)$$

Simulations

The model was simulated and the MoM equations in (3) were solved using the iterative AIM (iterative solver tolerance 10^{-4}), the direct $\mathcal{H}$-LU ($\tau_{\text{SVD}} = 10^{-3}$), and direct LU factorization algorithms. Even for this small problem, the fast algorithms required less computational resources than the classical approach; e.g., AIM required ~1/6th and $\mathcal{H}$-LU required ~1/3rd the memory compared to direct LU factorization. The real and imaginary parts of the received voltage computed using the different methods are plotted in Fig. 2 for two values of fracture conductivity. Figs. 2(a)–(b) show that the three algorithms yield results that agree well when $\sigma_{\text{V}} = 300\ \text{S/m}$ but the AIM approach fails to produce accurate results when $\sigma_{\text{V}} = 3000\ \text{S/m}$. Indeed, the iterative AIM algorithm requires more and more iterations for convergence as the fracture conductivity increases (Fig. 3) and eventually fails to converge. The fast direct solver, however, remains a viable approach for higher conductivity contrasts such that it can enable simulation of not only fractures with highly conductive proppant, but also anomalous regions of much higher conductivity, e.g., those typical to steel casings.

CONCLUSIONS

We introduced fast iterative and direct algorithms for the rigorous solution of 3D frequency-domain integral-equation formulations for subsurface geophysical applications. While fast iterative algorithms based on rapid matrix-vector multiplication methods are still unparalleled in terms of the size of problems they can solve, fast direct algorithms offer promising avenues for rapidly solving problems that challenge iterative solvers. Both classes of algorithms pave the way toward more robust inversion and interpretation of EM measurements from 3-D anomalies in subsurface sensing.
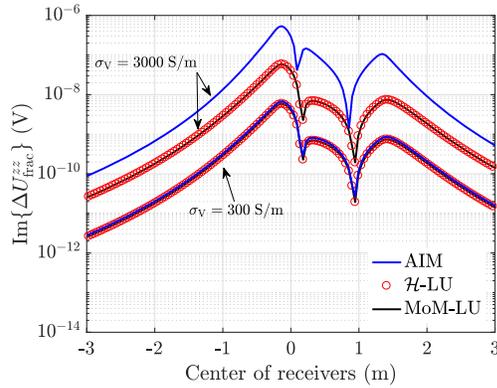
(a)
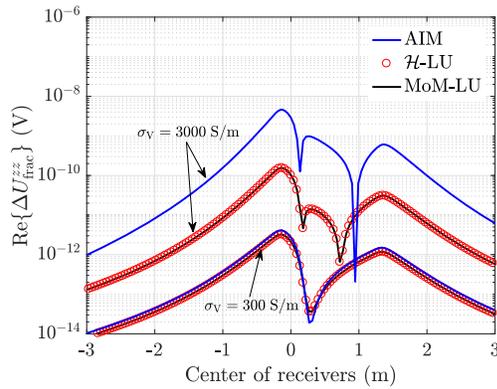
(b)

Figure 2. Imaginary and real parts of detected signals computed by the direct MoM, fast iterative AIM, and fast direct $\mathcal{H}$-LU algorithms.

Figure 3. Average number of iterations required by AIM with respect to fracture conductivity.

REFERENCES

Brick, Y., and Yilmaz, A. E., 2016, Fast multilevel computation of low-rank representation of $\mathcal{H}$-matrix blocks, *IEEE Trans. Antennas Prop.*, **64**, 5326–5334.

Fang, S., Gao, G.-Z., Torres-Verdin, C., 2006, Efficient 3D electromagnetic modelling in the presence of anisotropic conductive media, using integral equations, *Exploration Geophys.*, **37**, 239–244.

Hackbusch, W., 1999, A sparse matrix arithmetic based on $\mathcal{H}$-matrices. Part I: Introduction to $\mathcal{H}$-matrices, *Computing*, **62**, 89–108.

Hohmann, G. W., 1975, Three-dimensional induced polarization and electromagnetic modelling, *Geophysics*, **40**, 309–324.

Menshov, A., Yang, K., Okhmatovski, V., and Yilmaz, A., 2015, An $\mathcal{H}$-matrix accelerated direct solver for fast analysis of scattering from structures in layered media, *2015 USNC/URSI Radio Sci. Meeting*.

Menshov, A., Brick, Y., and Yilmaz, A. E., 2016, A fast direct integral-equation solver for hydraulic fracture diagnosis, *2016 USNC/URSI Radio Sci. Meeting*.
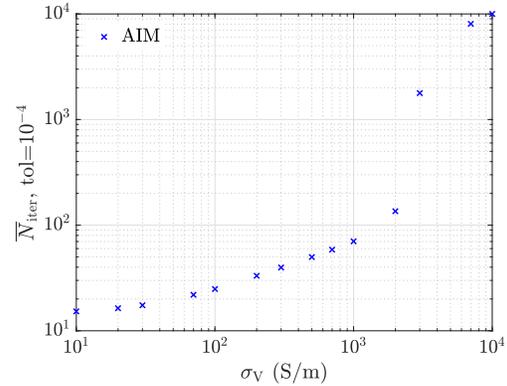
Nie, X.-C., Yuan, N., and Liu, C. R., 2010, Simulation of LWD tool response using a fast integral equation method, *IEEE Trans. Geo. Remote Sens.*, **48**, 72–81.

Nie, X. C., Yuan, N., and Liu, R., 2013, A fast integral equation solver for 3D induction well logging in formations with large conductivity contrasts, *Geophys. Prospect.*, **61**, 645–657.

Schaubert, D. H., Wilton, D. R., and Glisson, A. W., 1984, A tetrahedral modelling method for electromagnetic scattering by arbitrarily shaped inhomogeneous dielectric bodies, *IEEE Trans. Antennas Propag.*, **32**, 77–85.

Wei, F., and Yilmaz, A. E., 2014, A more scalable and efficient parallelization of the adaptive integral method part I: algorithm, *IEEE Trans. Antennas Propag.*, **62**, 714–726.

Yang, K., and Yilmaz, A. E., 2012, A three-dimensional adaptive integral method for scattering from structures embedded in layered media, *IEEE Trans. Geosci. Remote Sens.*, **50**, 1130–1139.

Yang, K., and Yilmaz, A. E., 2013, FFT-accelerated analysis of scattering from complex dielectrics embedded in uniaxial layered media, *IEEE Geosci. Remote Sens. Lett.*, **10**, 662–666.

Yang, K., Torres-Verdin, C., and Yilmaz, A. E., 2015, Detection and quantification of three-dimensional hydraulic fractures with horizontal borehole resistivity measurements, *IEEE Trans. Geosci. Remote Sens.*, **53**, 4605–4615.

Yu, Z., Zhang, W., and Liu, Q. H., 2014, A mixed-order stabilized bi-conjugate gradient FFT method for magnetodielectric objects, *IEEE Trans. Antennas Propag.*, **62**, 5647–5655.

Zhang, P., Shiriyev, J., Brick, Y. Massey, J., Torres-Verdin, C., Yilmaz, A. E., and Sharma, M., 2016, Fracture diagnostics using a low frequency electromagnetic induction method, *50th ARMA US Rock Mechanics/Geomechanics Symp.*